The TOP-2-condensin II axis silences transcription during germline specification in *C. elegans*

Mezmur D. Belew[1], Matthew Wong[1], Emilie Chien[1], and W. Matthew Michael[1*]

[1]Department of Biological Sciences, Molecular and Computational Biology Section, University of Southern California, Los Angeles, CA, 90089

[*]denotes corresponding author (mattm@usc.edu)

Abstract/Summary

In many organisms, mRNA transcription must be globally repressed in germline precursor cells during specification for them to maintain a germline fate. In *C. elegans*, germline precursor cells are known as the P lineage, and it is the PIE-1 protein that is responsible for silencing transcription in these cells. Loss of PIE-1 results in a fate switch, whereby the P2 cell loses germline fate and instead adopts a somatic fate. Previous work had also defined a global chromatin compaction (GCC) pathway that silences transcription in oocyte, spermatocytes, and primordial germ cells in *C. elegans*. GCC silencing requires the topoisomerase II (TOP-2)/condensin II chromatin compaction pathway together with components of H3K9me pathway. These factors come together to promote a global compaction of chromatin, thereby silencing gene expression. The goal of this study was to ask if the GCC pathway is also important for genome silencing in the P lineage. We report that GCC *per se* is not required, as we find that the H3K9me pathway is dispensable for transcriptional repression in P cells. However, we do uncover a critical role for TOP-2/condensin II in P-cell silencing. Loss of TOP-2 and/or the CAPG-

2 subunit of condensin II leads to active, elongating RNA polymerase II in P cells, leading to expression of both somatic and germline genes. These data shed new light on how transcription is regulated during germline specification.

Introduction

Just like individual genes, the transcriptional output of entire genomes can be regulated in a signal-mediated manner. In fact, genome repression and activation are recurring events during germline development and gametogenesis in the roundworm *C. elegans*. In meiotic prophase, for example, both oocytes and spermatocytes globally repress transcription as they prepare for the meiotic divisions (Walker et al, 2007; Belew et al, 2022). In both cases transcription is repressed by a global chromatin compaction (GCC) pathway (Belew et al, 2021; 2022), comprised of topoisomerase II, condensin II, and components of the H3K9me system. After fertilization, transcription remains repressed, but at this time repression is mediated by the OVA-1/2 proteins that bind to and inactivate the essential transcription factor TAF-4 (Guven-Ozkan et al, 2010). The OVA system blocks transcription through the first two mitotic divisions and then the proteins are rapidly degraded. Loss of OMA activates transcription in three of the four cells in the 4-cell embryo, with the holdout being the germline precursor P2. P2 remains transcriptionally repressed via the action of PIE-1, and this is the case for the remainder of P-lineage development (Mello et al, 1996; Seydoux et al, 1996; Dunn and Seydoux, 1997). Upon division of the P4 cell, to form the Z2/Z3 primordial germ cells (PGCs), PIE-1 is rapidly degraded and the germline robustly activates transcription for the first time (Mello et al, 1996; Schaner et al, 2003). Z2/Z3 are transcriptionally active for the remainder of embryogenesis, however if the embryo hatches into a nutrient-free environment then the PGC genome is rapidly silenced, and this requires the GCC pathway (Belew et al, 2021). Upon feeding, Z2/Z3 activate transcription again, in a manner that depends on the deposition of DNA breaks in the genome that allow the chromatin to decompact (Butuči et al, 2015; Wong et al,

2018). Thus, in summary, cells within the germline system shut down transcription during meiotic prophase by GCC, and repression is maintained first by OMA and then PIE-1. Transcription is activated in Z2/Z3 and then shut down again in starved L1s via GCC, and nutrients then allow for reactivation. What is remarkable about this system is the diversity of mechanisms used to repress transcription, from GCC to OMA to PIE-1 and then back to GCC again.

In this study we focused on transcriptional repression in early embryonic P-cells. The mechanism by which PIE-1 inhibits transcription is still poorly understood but has been linked to the phosphorylation of RNA polymerase II (RNAPII) on serines 2 and 5 within its carboxyl-terminal domain (CTD; Robert et al, 2015, Wang and Seydoux, 2013). The RNAPII CTD contains numerous copies of the heptapeptide repeat sequence $Y_1S_2P_3T_4S_5P_6S_7$, with humans containing 52 copies and nematodes 42 copies. During the transcription cycle, RNAPII arrives at the promoter in an unphosphorylated state and is then phosphorylated on serine 5 to allow promoter clearance. Phosphorylation on serine 2 follows, and this has been linked to an active, elongating state of RNAPII (reviewed in Zaborowska et al, 2016). PIE-1 blocks both serine 5 and serine 2 phosphorylation, and genetic experiments using separation-of-function mutants have shown that the ability to block serine 5 phosphorylation is critical to suppressing transcription in the P lineage, whereas the ability to block serine 2 phosphorylation is dispensable (Ghosh and Seydoux, 2008). How PIE-1 blocks serine 5 phosphorylation, mechanistically, is not understood. In this work we asked if the GCC pathway also plays a role in silencing transcription in P-cells, as it does in oocytes, spermatocytes, and the PGCs of starved L1s (Belew et al,

2021,2022). We find that the GCC per se is not required, as we found no role for the H3K9me pathway in silencing P-cell transcription. Interestingly, however, we do reveal a role for the TOP-2/condensin II axis in P-cell silencing. We report that loss of TOP-2/condensin II allows for activate, elongating RNAPII in P-cells, and we show that both somatic and germline genes are inappropriately transcribed. These data show that PIE-1 is not the whole story for silencing in the P-cell lineage, and they set the stage for detailed investigations into how TOP-2/condensin II blocks transcription, and whether they act with, or in parallel, to PIE-1.

Results and Discussion

Loss of TOP-2 and condensin II function results in active RNAPII in the P lineage of early embryos.

Previous work from our laboratory had defined the GCC pathway as a signal-mediated genome silencing system (Belew et al, 2021;2022), and thus we were interested in determining if GCC was active in the P-cells of early embryos, which are known to be transcriptionally repressed (Robert et al, 2015, Wang and Seydoux, 2013). To do so, we stained early embryos with an antibody that detects a phospho-serine 2 on the RNAPII CTD (referred to as RNAPIIpSer2 for the remainder of this study). The presence of RNAPIIpSer2 signal has been used as a marker for actively elongating RNA polymerase II (Palancade and Bensaude, 2003), and we and others have used this approach extensively to identify transcriptionally active nuclei within a variety of *C. elegans* tissues (Dunn and Seydoux, 1997; Walker et al, 2004; Wong et al, 2018; Belew et al, 2021;2022). The antibody that we are using, a rabbit polyclonal that recognizes RNAPIIpSer2, has previously been validated by us for use in *C. elegans* embryos (Belew et al, 2021). We first examined zygotes and 2-cell embryos that had been exposed to either control RNAi or RNAi against two different components of the GCC pathway, *top-2* or *set-25*. As expected, the control RNAi samples did not show any RNAPIIpSer2 signal, in either zygotes or 2-cell samples, and the same was true of the *top-2* RNAi and *set-25* RNAi samples (Figure S1). We conclude that the GCC pathway is not involved in transcriptional repression in very early, one- and two-cell embryos embryos.

It is at the 4-cell stage that the somatic precursor cells ABa, ABp, and EMS activate zygotic transcription (Seydoux and Fire, 1994). The remaining cell, P2, remains transcriptionally repressed due to the presence of PIE-1. We stained 4-cell embryos for RNAPIIpSer2 and for the control samples the expected pattern emerged – signal could be seen in ABa, ABp, and EMS, but not P2 (Figure 1). Interestingly, in samples exposed to either *top-2* or *capg-2* RNAi, we could now detect RNAPIIpSer2 in P2, and the same was true of samples exposed to *pie-1* RNAi (Figure 1). We next examined the remainder of the P-lineage (P3 and P4) and in both cases we could detect active transcription after depletion of either TOP-2, CAPG-2, or PIE-1 (Figure 1). Based on these data we conclude that TOP-2 and condensin II are dispensable for transcriptional repression in P0 and P1, but for P2, P3, and P4 they are required to silence gene expression.

Aberrant expression of both somatic and germline genes is observed in the P-lineage when TOP-2 and condensin II are depleted.

Data presented thus far demonstrate aberrant transcriptional activity in P2, P3, and P4 after depletion of TOP-2 or CAPG-2. To obtain additional evidence for the misregulation of gene expression in these cells, we performed the *in situ* hybridization chain reaction (HCR), also known as RNA-FISH (Choi et al, 2016), to detect and localize mRNAs in early embryos. For this, we focused on 4-cell embryos, and we started by looking at the expression pattern of the somatic gene *vet-6*, which has previously been shown to be expressed exclusively in EMS at the 4-cell stage (Seydoux et al., 1996). In wild-type embryos, *vet-6* expression was indeed localized to the EMS blastomere, with 100% of samples showing *vet-6* transcript signals in EMS. On the

other hand, only 7.5% of wild-type embryos had *vet-6* signal in P2. Upon treatment with *top-2* RNAi, however, most of the samples (57.5%) had *vet-6* transcripts in P2 (Figure 2A). We also examined the expression pattern of an additional transcript, F58E6.6. Similar to *vet-6*, F58E6.6 transcripts are seen predominantly in EMS in wild-type embryos, with only 10-20% of our wild-type samples showing transcript signals in ABa, ABp, or P2. After TOP-2 or CAPG-2 depletion, however, 50% and 82%, respectively, of the P2 cells examined were now expressing F58E6.6 (Figure BB and S2A&B). As a positive control, we depleted PIE-1 and found that both *vet-6* and F58E6.6 transcripts were expressed in P2 in 85% and 100% of our samples (Figures 2A and S2B&C). We conclude that depletion of TOP-2 and condensin II results in the misexpression of somatic genes in the P-lineage of early embryos. To pursue these observations, we next examined germline gene expression in early embryos after depletion of TOP-2 or CAPG-2. The *ppw-2* gene is normally expressed in the Z2/Z3 PGCs of late embryos, but not in P2 of early embryos (Figure 3). After depletion of either TOP-2 or CAPG-2, however, we could readily observe expression of *ppw-2* in P2 (Figure 3). Taken together the data in Figures 1-3 show that the TOP-2/condensin II axis is required to repress transcription in the P-lineage, and that both somatic and germline genes are misexpressed when TOP-2/condensin II function is compromised.

The H3K9me pathway is dispensable for genome silencing in the P-lineage.

Data thus far have focused on the role of TOP-2/condensin II in transcriptional control within the P-lineage. For the GCC pathway, TOP-2 and condensin II collaborate with the

H3K9me pathway to repress transcription, and thus we next explored the possibility that H3K9me pathway components are operational during P-lineage silencing. One characteristic of GCC-mediated silencing is the massive accumulation of H3K9me3 marks on chromatin, and this is observed in Z2/Z3 of late embryos, in starved L1s, and in pre-maturation oocytes (Belew et al, 2021;2022). To determine if H3K9me marks also accumulate in transcriptionally silenced cells of the P-lineage we stained early embryos for H3K9me3. Figure 4A shows representative images for both early and late zygotes. Importantly, we have previously shown that the chromatin of pre-fertilization oocytes is heavily decorated with H3K9me3 marks, such that the immunofluorescence signal for H3K9me3 overlaps entirely with the DNA-based DAPI signal (Belew et al, 2022). This is not the case for nuclei in one-cell embryos, where H3K9me3 signal is present, but is limited to small patches scattered along the chromosomes (Figure 4A). By contrast, H3K9me3 signals are much stronger on polar bodies, where they overlap with much of the DAPI signal. These data suggest that, upon fertilization, H3K9me3 marks are rapidly erased on much of the chromatin inside the female pronucleus, but not on the chromatin in polar bodies. We went on to examine 4- and 8-cell embryos, comparing P2 and P3 to their sister cells EMS and C. All four cell types showed a similar pattern of H3K9me3 foci scattered throughout the chromatin, and quantification of these signals showed that P cells did not accumulate H3K9me3 marks to a greater extent than their transcriptionally active sisters (Figure 4B). Consistent with a lack of massive accumulation of H3K9me3 marks in the P-lineage we also observed that *set-25* mutant embryos could readily silence transcription in the P-lineage, as assessed by RNAPIIpSer2 staining (Figure 4C). In both oocytes and starved L1s the SET-25 methyltransferase plays a crucial role in genome silencing (Belew et al, 2021, 2022). Based on

these data we conclude that GCC pathway *per se* is not required for genome silencing in the P-lineage, and thus that TOP-2 and condensin II mediate silencing in a manner independent of heterochromatin assembly.

Transcriptome analysis of TOP-2/CAPG-2 depleted early embryos.

Having established that TOP-2/condensin II controls gene expression in the early embryonic P-lineage we moved on to determine to what extent transcription is deregulated in early embryos upon loss of these factors. For this we performed RNA-seq analysis on control or *top-2/capg-2* depleted early embryos. L1 larvae were synchronized by hatching in minimal media and then plated on food. Growth was monitored such that as soon as young adults had formed embryos the samples were bleached and early embryos were purified and used for RNA extraction. The transcriptomes were then sequenced in replicate and principal component analysis revealed that replicates of the *top-2/capg-2* RNAi treated samples cluster away from those of the control treated samples, confirming RNAi treatment underlies the separation among the samples (Figure 5A). Moreover, using an adjusted p-value cutoff of 0.05, we found 316 differentially expressed genes (DEGs) in the *top-2/capg-2* RNAi samples, with 144 of them upregulated and 172 downregulated (Figure 5B, Supplemental Table 1). The fact that more than half of the DEGs are downregulated was surprising, given the repressive nature of TOP-2 and condensin II (Belew et al., 2021; Swygert et al., 2019). A possible cause for this could be the misexpression of repressor genes due to loss of TOP-2 and condensin II which, in turn, would result in the downregulation of the genes in our experiment. A deeper analysis of the DEGs

revealed that they were evenly distributed among the six C. elegans chromosomes, implying the occurrence of genome-wide misexpression without a bias towards a single chromosome (data not shown).

To pursue these observations we wanted to validate our findings from the RNA sequencing experiment using a second set of independent experiments. To do so, we picked three genes that are upregulated in our *top-2/capg-2* RNAi samples (*zip-2*, *cab-1*, and *asns-2*) and performed *in situ* HCR to visualize their expression patterns in early embryos. We started our investigation by looking at 4- and 8-cell embryos and found that wild-type embryos had very little to no HCR signal. However, upon the depletion of TOP-2 and CAPG-2, we saw a pan-embryonic increase in transcripts for all three genes (Figure 6A-C). We then asked if the increase in transcripts is due to novel transcription taking place in early embryos. We reasoned that if so, we would not detect any transcripts in very early (i.e., 1- and 2-cell) embryos, as those embryos harbored no detectable pSer2 signal (Figure S1). Interestingly, we saw an increase in HCR signal in *top-2/capg-2* RNAi treated very early embryos, similar to what we observed when we analyzed 4- and 8-cell embryos (Figure 7A-C). With these findings in mind, we conclude that the misexpression of genes is initiated in oocytes, and those transcripts are loaded into early embryos. But it is also important to note that we cannot completely rule out the possibility that novel transcription is taking place during early embryogenesis when TOP-2 and condensin II functions are lost. Nonetheless, the HCR data in Figures 6 and 7 validates our list of DEGs.

We next analyzed our group of 144 upregulated genes to search for commonality. Gene enrichment analysis was performed and we observed that many of the genes (22 in total) shared gene ontology (GO) terms related to defense and interspecies interactions (Figure 8A), and this group includes the *zip-2* gene that was the subject of the HCR analysis in Figures 6 and 7. For tissue distribution, most of the enrichment we observed was for the nervous system, as SIB, ALA, DVB, and SIA are all neurons (Figure 8B). Next, we compared our dataset to other previously published datasets to get more information regarding our DEGs. First, because TOP-2/condensin II work together in the GCC pathway with the SET-25 and MET-2 methyltransferases, we compared our list of upregulated genes to a list of genes that are upregulated in *set-25, met-2* double mutant early embryos that was produced by Gasser and colleagues (Zeller et al, 2016). The two groups had just 5 genes in common (Figure 8C), suggesting that TOP-2/condensin II acts independently of the H3K9me pathway is early embryos, and this is consistent with the lack of involvement of SET-25 in repressing transcription in P cells (Figure 6). Similarly, we observed scant overlap with gene sets that are provided maternally to early embryos (Figure 8D), or with genes that are expressed in the gonad (Figure 8E). By contrast, strong overlap was observed with genes that are expressed somatically (Figure 8F). All together, our transcriptome analysis strongly suggests that the TOP-2/condensin II axis does not regulate transcription at the level of individual genes, as we identified just 316 DEGs after depletion of TOP-2 and CAPG-2. That said, there may be a role for TOP-2/condensin II in coordinately repressing genes involved in the defense response, in either oocytes or early embryos. Overall, we propose that TOP-2/condensin II plays a more substantial

role in the global silencing of gene expression than it does in regulating individual gene expression.

In this study we asked if the GCC pathway, known to silence the genomes of oocytes, spermatocytes, and PGCs, also silences gene expression in P cells during germline specification. The answer was clear, that GCC per se is not involved, as some of the hallmarks of GCC events – e.g. the massive accumulation of H3K9me marks, a requirement for SET-25 in silencing, and most notably extreme chromatin compaction – are not occurring in P cells. We did, however, reveal a role for TOP-2/condensin II in genome silencing during germline specification. It thus appears that TOP-2/condensin II can work independently of the H3K9me pathway in regulating transcription on a global level. Previous work had identified PIE-1 as required for genome silencing in P2, P3, and P4, and thus TOP-2 and condensin II are just the second and third factors to be identified that perform this crucial function. One fascinating question that arises from our findings is the relationship between PIE-1 and TOP-2/condensin II. Do these factors form a single, linear pathway for genome silencing, or are they acting independently of one another? Further work is needed to answer this important question, and such experiments are now in progress.

Materials and Methods

C. elegans strains

N2 (wild-type), SS747 bnIs1[pie-1::GFP::pgl-1 + unc-119(+)], WMM1 ([pie-1::gfp::pgl-1 + unc-119(+)]; [(pAA64)pie-1p::mCherry::his-58 + unc-119(+)] IV), and MT17463 (set-25(n5021) III) strains were used in this study. Worms were maintained on 60mm plates containing nematode growth media (NGM) seeded with the *E. coli* strain OP50 or HT115. Worms were grown at 20°C and propagated through egg preparation (bleaching) every 72 hours.

Bacterial strains

OP50 bacteria served as the primary food source. It was grown in LB media containing 100 ug/ml streptomycin by shaking at 37°C overnight. 500 ul of the culture was seeded on Petri-dishes containing NGM + streptomycin. HT115 bacteria grown in LB media containing 100 ug/ml carbenicillin and 12.5 ug/ml tetracycline and seeded on NGM + carbenicillin + tetracycline plates were also used as a source of food. Our RNAi strains were obtained from the Ahringer library and verified by Sanger sequencing. Bacteria containing dsRNA were streaked on LB-agar plates containing 100 ug/ml carbenicillin and 12.5 ug/ml tetracycline and incubated at 37°C overnight. Single colonies were then picked and grown in 25ml LB cultures with 100 ug/ml carbenicillin and 12.5 ug/ml tetracycline. 500 ul of this culture was seeded on 60 mm Petri-dishes containing 5mM IPTG.

Egg preparation

Bleach solution containing 3.675 ml H2O, 1.2 NaOCl, and 0.125 ml 10N NaOH was prepared. Adult worms were washed from plates with 5 ml of M9 minimal medium (22mM KH2PO4, 22mM Na2HPO4,

85mM NaCl, and 2mM MgSO4). Worms were centrifuged at 1.9 KRPM for 1 minute and the excess medium was removed, then the bleach solution was added. Eggs were extracted by vortexing for 30 seconds and shaking for 1 minute. This was done a total of 3 times and worms were vortexed one last time. Then the eggs were spun down at 1900 rpm for 1 minute and excess bleach solution was removed and the eggs were washed 3 times with M9 minimal medium.

RNAi treatment

RNAi containing NGM plates were prepared as described in the "Bacterial strains" section. For double RNAi treatments, RNAi cultures were mixed at a 1:1 ratio by volume. HT115 cells transformed with an empty pL4440 vector was used as a negative control. RNAi conditions used in this study and tests for their efficacy is described below:

<u>*top-2* RNAi</u>

L1 worms were plated on HT115 food plates for the first 24 hours and were then moved to plates seeded with *top-2* RNAi for the remaining 48 hours. Embryonic lethality was observed at >90%.

<u>*capg-2* RNAi</u>

Worms were grown on HT115 food plates for the first 24 hours and were moved to plates containing *capg-2* RNAi for the remaining 48 hours. An embryonic lethality of 80%-100% was seen with this RNAi treatment.

<u>*top-2/capg-2* double RNAi</u>

Worms were grown on HT115 food plates for the first 24 hours and were transferred to *top-2/capg-2* double RNAi plates for the next 48 hours. Embryonic lethality ranged from 90%-100% for this RNAi treatment.

set-25 RNAi

Worms were grown on plates containing *set-25* RNAi for the entirety of their life cycle. Some of the adult worms were bleached and an L1 chromatin compaction assay was performed on the resulting larvae to test RNAi efficacy. Please see Belew et al., 2021, for details on the L1 compaction assay.

pie-1 RNAi

Worms were grown on plates containing *pie-1* RNAi for the entirety of their life cycle.

Antibodies and dilutions

RNAPIIpSer2: Rabbit antibody from Abcam (ab5095, Cambridge, Massachusetts) was used at a dilution of 1:100. GFP: mouse Mab #3580, from EMD Millipore, was used at 1:500. H3K9me3: Rabbit antibody from Abcam (ab176916, Cambridge, Massachusetts) was used at a dilution of 1:1000. P-granules: mouse Mab K76, from the Developmental Studies Hybridoma Bank, was used neat. Secondary antibodies: Alexa Fluor conjugated secondary antibodies from Invitrogen (Thermofisher Scientific, Waltham, Massachusetts) were used at a dilution of 1:200.

Immunofluorescence staining

Adult worms were first washed off plates with 10 ml of M9 minimal medium and washed 3 more times. Then, they were centrifuged at 1.9 KRPM and the excess medium was removed. 20 ul of media

containing about 50 worms were spotted on a coverslip and 3 ul of anesthetic (20mM Sodium Azide and 0.8M Tetramisole hydrochloride) was added to immobilize them. Worms were dissected using 25Gx5/8 needles (Sigma Aldrich, St. Louis, Missouri). To release gonads, adult worms were cut twice, once right below their pharyngeal bulb and once near the tail. The coverslip was then mounted onto poly-L-lysine covered slides and let rest for 5 minutes. Slides were put on dry ice for 30 minutes. Samples were then freeze-cracked by flicking the coverslips off for permeabilization.

For RNAPIIpSer2 staining experiments, once samples are permeabilized, slides were put in cold 100% methanol for 2 minutes and then fixing solution (0.08M HEPES pH 6.9, 1.6mM MgSO4, 0.8mM EGTA, 3.7% formaldehyde, 1X phosphate-buffered saline) for another 30 minutes. After fixing, slides were washed three times with TBS-T (TBS with 0.1% Tween-20) and were blocked for 30 minutes with TNB (containing 100mM Tris-HCl, 200 mM NaCl, and 1% BSA). Primary antibodies were then applied at the dilutions described above in TNB and slides were incubated at 4°C overnight.

For H3K9me3 staining experiments, permeabilized samples were put in cold 100% methanol for 10 seconds and then fixing solution (0.08M HEPES pH 6.9, 1.6mM MgSO4, 0.8mM EGTA, 3.7% formaldehyde, 1X phosphate-buffered saline) for 10 minutes. After fixing, slides were washed three times with TBS-T (TBS with 0.1% Tween-20) and were blocked for 2 hours with TNB (containing 100mM Tris-HCl, 200 mM NaCl, and 1% BSA) supplemented with 10% goat serum. Primary antibodies were then applied at the dilutions described above in TNB and slides were incubated at 4°C overnight.

On the next day, the slides were washed 3 times with TBS and slides were incubated with secondary antibodies and Hoechst 33342 dye for 2 hours at room temperature. Slides were washed 3 times with TBS, mounting medium (50 % glycerol in PBS), and coverslips were applied and sealed with Cytoseal XYL (Thermofisher).

HCR (In Situ Hybridization Chain Reaction)

A kit containing a DNA probe set, DNA hybridized chain reaction (HCR) amplifier hairpins, and hybridization, wash, and amplification buffers were purchased from Molecular Instruments (molecularinstruments.com). Genes that were examined were vet-6, F58E6.6, ppw-2, cab-1, zip-2, and asns-2. DNA was visualized with Hoechst 33342 dye. Embryos were prepared by bleaching and were immediately spotted on poly-L-lysine coated slides. Coverslips were applied and slides were freeze-cracked to permeabilize samples. Immediately after freeze-cracking, 500 ul of 100% ice-cold methanol was applied over the samples. Slides were dried off by tilting slides, 1 ml of 4% paraformaldehyde (PFA) was added and samples were incubated in a humidity chamber for 10 minutes. Samples were then washed 3 times with 100 ul of PBS-T. A 1:1 solution of probe hybridization buffer (PHB) and PBS-T was added to the samples, and they were incubated for 5 minutes at room temperature. Samples were then prehybridized with PHB for 30 minutes at 37oC and DNA probes (at a final concentration of 2 picomoles per 500 ul of PHB) were added to the samples and were incubated overnight at 37oC.

The next day, samples were washed 4 times with probe wash buffer (PWB) at 37oC with 15 minutes of incubation for each wash. They were then washed three more times with 5xSSCT at room temperature. Samples were pre-amplified with Amplification buffer for 30 minutes at room temperature. Probe amplifier hairpins were snap cooled by heating to 95oC for 90 seconds and putting in a dark drawer for 30 mins then were added to the sample. Worms were incubated with the hairpins overnight in a dark drawer.

On the third day, samples were washed with 5xSSCT and incubated with Hoechst-33342 (1:5000 dilution) for 15 minutes. Finally, samples were mounted on poly-L-lysine coated slides and imaged.

Immunofluorescent imaging

All slides were imaged using an Olympus Fluoview FV1000 confocal microscope using Fluoview Viewer software. Laser intensity was controlled for experiments to achieve consistency among samples.

RNA isolation for sequencing

Embryos were synchronized by bleaching young adults as soon as the first eggs were seen in the animal to enrich for early embryos (Boeck et al., 2016). This was done on three successive generations to tighten the synchrony. After the final round of bleaching, the embryos were washed with 10 ml cold M9 minimal medium and packed by centrifuging at 1.9 KRPM. A portion of the sample was taken to assess the stage of the embryos by staining DNA. The rest of the embryos were flash-frozen in liquid nitrogen and stored at -80oC until the RNA isolation step.

Samples were thawed and four volumes of Tri-reagent (Sigma Aldrich, St. Louis, Missouri) were added to them. The mixture was then vortexed vigorously to solubilize the embryos. Once solubilized, the sample was distributed into Eppendorf tubes by adding 1250 ul of the sample to each tube. Samples were incubated for 5 minutes at room temperature and centrifuged at 14 KRPM for 10 minutes at 4oC to remove debris. The supernatant was then transferred into fresh tubes and 200 ul of Chloroform (Sigma Aldrich, St. Louis, Missouri) was added to each tube. The solution was vortexed for 15 seconds and incubated at room temperature for 3 minutes before being centrifuged at 14 KRPM and 4oC for 15 minutes. The top aqueous layer was carefully transferred to new centrifuge tubes and 500 ul of isopropanol (Sigma Aldrich, St. Louis, Missouri) was added to it. This mixture was incubated at room temperature for 10 minutes and then centrifuged for 10 minutes at 14 KRPM and 4oC to precipitate RNA. The supernatant was discarded, and the pellet was washed with 100 ul of 75% EtOH in diethyl pyrocarbonate (DEPC) treated water. The sample was then centrifuged one more time at 7.5 KRPM for 5 minutes at 4oC, the supernatant was removed, and the pellet was air-dried in a fume hood for 15

minutes. Finally, the dry pellet was dissolved in 50 ul of DEPC treated water and sent to Genewiz (South Plainfield, NJ) for library preparation and sequencing. This was repeated for a second biological replicate.

RNA sequencing data analysis

Library preparation and sequencing were done by Genewiz (South Plainfield, NJ). Fastq files were imported into Partek-flow. Prior to alignment, reads were assessed for sequencing quality and bases with quality score less than 20 were trimmed. If a read had a length lower than 25 bp after trimming the whole read was discarded. STAR aligner was used to align reads to *C. elegans* – WB235 assembly which was retrieved from WormBase. After alignment, reads were quantified using the Partek-EM method to WB235manual-Ensembl104 annotation model that is also available on WormBase. Genes whose counts across all samples were less than 50 were filtered out and then gene counts were normalized using the median ratio method for DEseq2. Finally, DEseq2 was used to generate a list of differentially expressed genes.

Upon getting the list of differentially expressed genes, we set an adjusted P-value cutoff of 0.05 to attribute statistical significance. A fold-change cutoff of -1 and 1 was used to identify genes that were downregulated and upregulated, respectively. The “ggplot2” package was on R used to construct a volcano plot to visualize these genes. Principal component analysis to see the separation of our samples was done using R and was visualized using the “ggplot2” package. The “Gene set enrichment analysis” tool on WormBase was used to identify tissues and biological processes that were enriched in our upregulated genes. A short R script that cross-checks our list of upregulated genes against lists of genes from various studies for similarities was written to perform the overlap analyses presented in this study.

References

Belew MD, Chien E, Wong M, Michael WM. A global chromatin compaction pathway that represses germline gene expression during starvation. J Cell Biol. 2021 Sep 6;220(9):e202009197. doi: 10.1083/jcb.202009197.

Belew MD, Chien E, Wong M, Michael WM. The global chromatin compaction pathway silences transcription during meiotic prophase in C. elegans. BioRxiv. 2022 Aug 28; 505591. doi: 10.1101/2022.08.28.505591.

Boeck ME, Huynh C, Gevirtzman L, Thompson OA, Wang G, Kasper DM, Reinke V, Hillier LW, Waterston RH. The time-resolved transcriptome of C. elegans. Genome Res. 2016 Oct;26(10):1441-1450. doi: 10.1101/gr.202663.115.

Butuči M, Williams AB, Wong MM, Kramer B, Michael WM. Zygotic Genome Activation Triggers Chromosome Damage and Checkpoint Signaling in C. elegans Primordial Germ Cells. Dev Cell. 2015 Jul 6;34(1):85-95. doi: 10.1016/j.devcel.2015.04.019.

Choi HM, Calvert CR, Husain N, Huss D, Barsi JC, Deverman BE, Hunter RC, Kato M, Lee SM, Abelin AC, Rosenthal AZ, Akbari OS, Li Y, Hay BA, Sternberg PW, Patterson PH, Davidson EH, Mazmanian SK, Prober DA, van de Rijn M, Leadbetter JR, Newman DK, Readhead C, Bronner ME, Wold B, Lansford R, Sauka-Spengler T, Fraser SE, Pierce NA. Mapping a multiplexed zoo of mRNA expression. Development. 2016 Oct 1;143(19):3632-3637. doi: 10.1242/dev.140137.

Ghosh D, Seydoux G. Inhibition of transcription by the Caenorhabditis elegans germline protein PIE-1: genetic evidence for distinct mechanisms targeting initiation and elongation. Genetics. 2008 Jan;178(1):235-43. doi: 10.1534/genetics.107.083212.

Mello CC, Schubert C, Draper B, Zhang W, Lobel R, Priess JR. The PIE-1 protein and germline specification in C. elegans embryos. Nature. 1996 Aug 22;382(6593):710-2. doi: 10.1038/382710a0.

Palancade B, Bensaude O. Investigating RNA polymerase II carboxyl-terminal domain (CTD) phosphorylation. Eur J Biochem. 2003 Oct;270(19):3859-70. doi: 10.1046/j.1432-1033.2003.03794.x.

Quarato P, Singh M, Cornes E, Li B, Bourdon L, Mueller F, Didier C, Cecere G. Germline inherited small RNAs facilitate the clearance of untranslated maternal mRNAs in C. elegans embryos. Nat Commun. 2021 Mar 4;12(1):1441. doi: 10.1038/s41467-021-21691-6.

Reed KJ, Svendsen JM, Brown KC, Montgomery BE, Marks TN, Vijayasarathy T, Parker DM, Nishimura EO, Updike DL, Montgomery TA. Widespread roles for piRNAs and WAGO-class siRNAs in shaping the germline transcriptome of Caenorhabditis elegans. Nucleic Acids Res. 2020 Feb 28;48(4):1811-1827. doi: 10.1093/nar/gkz1178.

Robert VJ, Garvis S, Palladino F. Repression of somatic cell fate in the germline. Cell Mol Life Sci. 2015 Oct;72(19):3599-620. doi: 10.1007/s00018-015-1942-y.

Schaner CE, Deshpande G, Schedl PD, Kelly WG. A conserved chromatin architecture marks and maintains the restricted germ cell lineage in worms and flies. Dev Cell. 2003 Nov;5(5):747-57. doi: 10.1016/s1534-5807(03)00327-7.

Seydoux G, Fire A. Soma-germline asymmetry in the distributions of embryonic RNAs in Caenorhabditis elegans. Development. 1994 Oct;120(10):2823-34. doi: 10.1242/dev.120.10.2823.

Seydoux G, Mello CC, Pettitt J, Wood WB, Priess JR, Fire A. Repression of gene expression in the embryonic germ lineage of C. elegans. Nature. 1996 Aug 22;382(6593):713-6. doi: 10.1038/382713a0.

Seydoux G, Dunn MA. Transcriptionally repressed germ cells lack a subpopulation of phosphorylated RNA polymerase II in early embryos of Caenorhabditis elegans and Drosophila melanogaster. Development. 1997 Jun;124(11):2191-201. doi: 10.1242/dev.124.11.2191.

Swygert SG, Kim S, Wu X, Fu T, Hsieh TH, Rando OJ, Eisenman RN, Shendure J, McKnight JN, Tsukiyama T. Condensin-Dependent Chromatin Compaction Represses Transcription Globally during Quiescence. Mol Cell. 2019 Feb 7;73(3):533-546.e4. doi: 10.1016/j.molcel.2018.11.020.

Walker AK, Boag PR, Blackwell TK. Transcription reactivation steps stimulated by oocyte maturation in C. elegans. Dev Biol. 2007 Apr 1;304(1):382-93. doi: 10.1016/j.ydbio.2006.12.039.

Wang JT, Seydoux G. Germ cell specification. Adv Exp Med Biol. 2013;757:17-39. doi: 10.1007/978-1-4614-4015-4_2.

Wong MM, Belew MD, Kwieraga A, Nhan JD, Michael WM. Programmed DNA Breaks Activate the Germline Genome in Caenorhabditis elegans. Dev Cell. 2018 Aug 6;46(3):302-315.e5. doi: 10.1016/j.devcel.2018.07.002.

Zaborowska J, Egloff S, Murphy S. The pol II CTD: new twists in the tail. Nat Struct Mol Biol. 2016 Sep 6;23(9):771-7. doi: 10.1038/nsmb.3285. PMID: 27605205.

Zeller P, Padeken J, van Schendel R, Kalck V, Tijsterman M, Gasser SM. Histone H3K9 methylation is dispensable for Caenorhabditis elegans development but suppresses RNA:DNA hybrid-associated repeat instability. Nat Genet. 2016 Nov;48(11):1385-1395. doi: 10.1038/ng.3672.

Funding

This work was funded by a grant from the National Institutes of Health (R01GM127477) to W.M.M.

Author Contributions

W.M.M. acquired funding and conceptualized the project. W.M.M designed experiments. M.D.B., M.M.W., E.C., and W.M.M. performed experiments. W.M.M. and M.D.B. wrote the manuscript.

Declaration of interests

The authors declare no competing interests.

1 **Figure Legends**

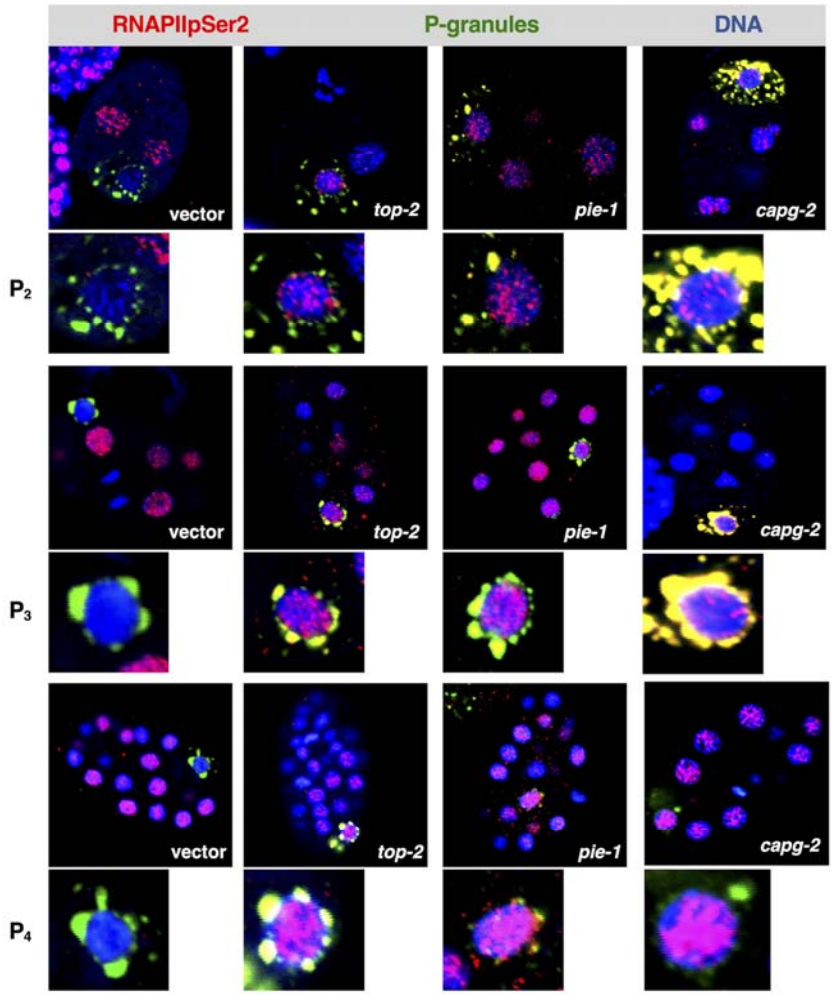

pSer2-postive P_2 after given RNAi:

vector	0/62	0%
top-2	23/41	56.1%
pie-1	9/13	69.2%
capg-2	5/18	27.8%

pSer2-postive P_3 after given RNAi:

vector	1/87	1.1%
top-2	26/52	50%
pie-1	17/18	94.4%
capg-2	16/40	40%

pSer2-postive P_4 after given RNAi:

vector	6/89	6.7%
top-2	26/45	57.8%
pie-1	14/15	93.3%
capg-2	22/42	52.4%

2

3 **Figure 1**: Loss of TOP-2 or CAPG-2 allows for active RNAPII in the P-lineage of early embryos.

4 Early embryos from N2 worms treated with control, *top-2*, *capg-2* or *pie-1* RNAi were fixed and

5 stained for P-granules (green), RNAPIIpSer2 (red) and DNA (blue). Shown on top are the entire

6 embryos and the P-cell is magnified below. Quantification of the data is shown at right.

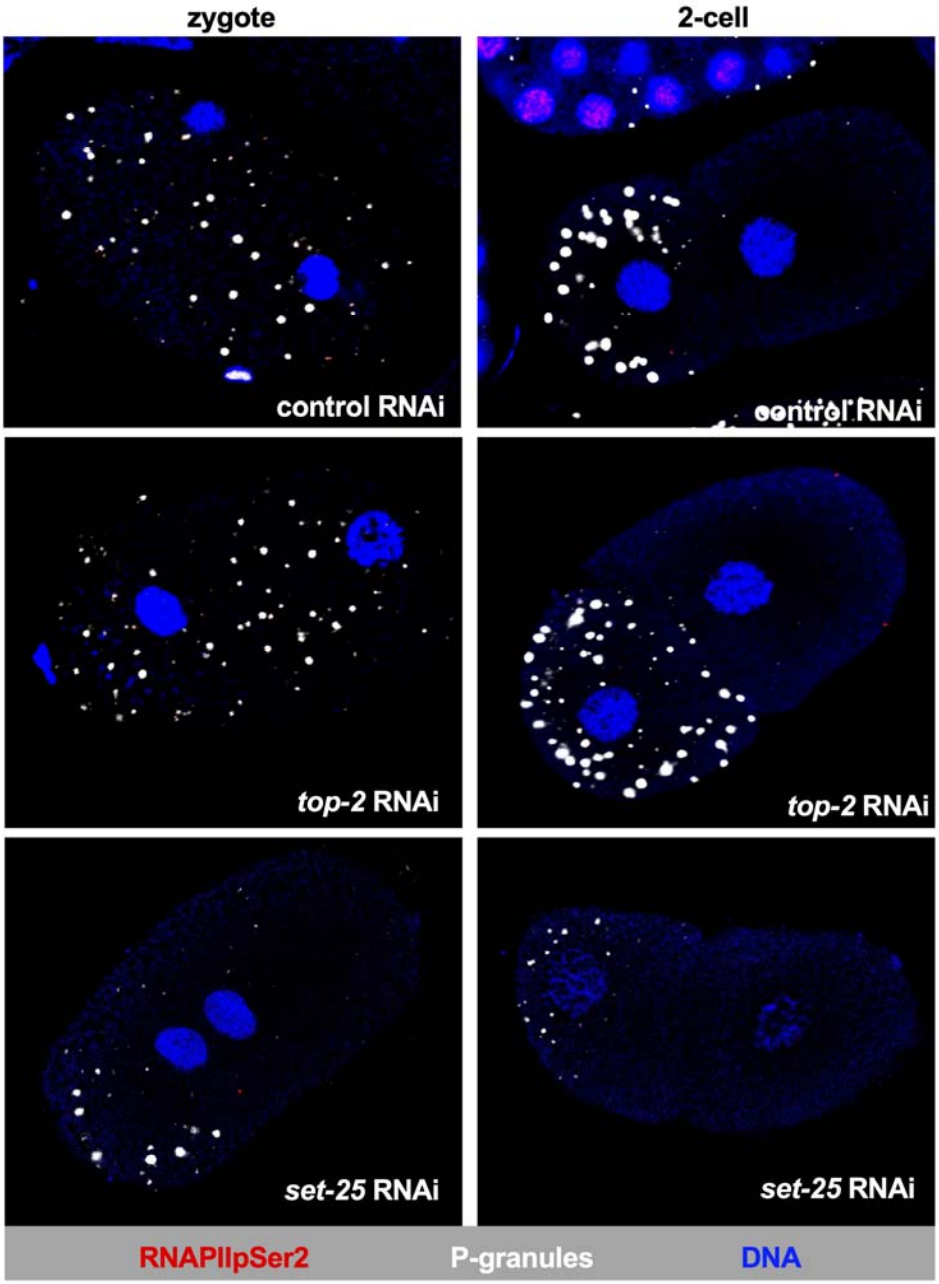

Figure S1: RNAPII-mediated transcription is still repressed in one- and two-cell embryos after loss of TOP-2 or SET-25.

One- and two-cell embryos from WMM1 worms treated with the indicated RNAi were fixed and stained for P-granules (white), RNAPIIpSer2 (red) and DNA (blue). No active RNAPII was

observed in the more than 20 samples we examined for both one- and two-cell embryos. Note the RNAPIIpSer2 signals in the adjacent, older embryo in the upper right panel – this shows that the staining worked efficiently.

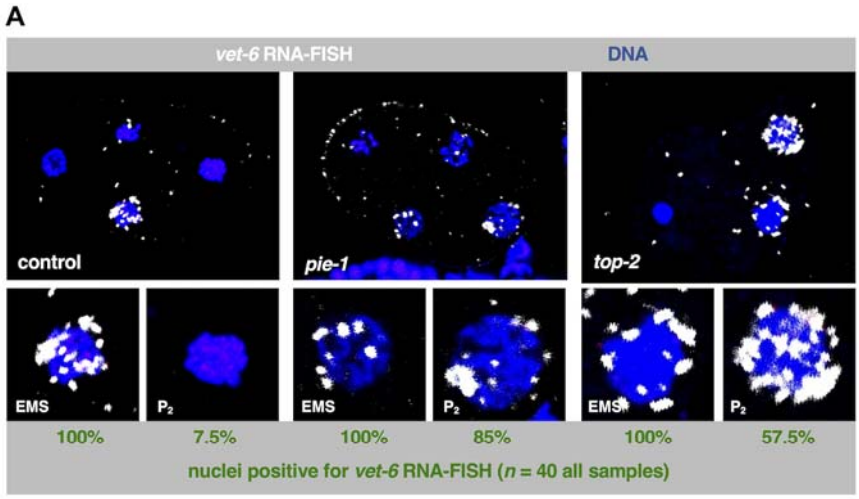

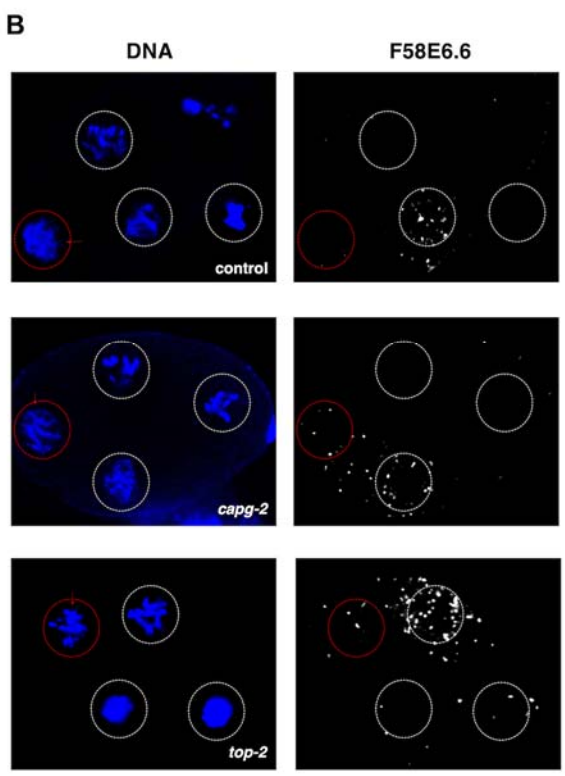

F58E6.6 transcript present in:

P_2	EMS	ABp	ABa
Y	Y	N	N
N	Y	N	N
Y	Y	N	N
N	Y	N	N
N	Y	N	N
N	Y	Y	Y
N	Y	N	N
N	Y	Y	N
N	Y	N	N
N	Y	N	N
2/10 Y	10/10 Y	2/10 Y	1/10 Y
Y	Y	N	N
Y	Y	N	Y
Y	Y	N	N
N	Y	N	N
N	Y	N	N
Y	Y	N	N
Y	Y	N	Y
Y	Y	N	N
Y	Y	N	N
Y	Y	N	N
9/11 Y	11/11 Y	0/11 Y	2/11 Y
N	Y	N	Y
Y	Y	N	N
N	Y	N	N
Y	Y	Y	Y
N	Y	Y	Y
N	Y	Y	N
N	Y	N	N
Y	Y	N	N
Y	Y	Y	Y
Y	Y	N	N
5/10 Y	10/10 Y	4/10 Y	4/10 Y

Figure 2: Somatic genes are aberrantly expressed in the P2 cell of 4-cell embryos after loss of TOP-2 or CAPG-2.

A. 4-cell embryos from N2 animals treated with control, *top-2* or *pie-1* RNAi were fixed and HCR was performed to probe for *vet-6* mRNA (white) and DNA (blue). Representative images are

shown and percentage of samples with *vet-6* transcripts in P2 are shown below (n=40). **B.** 4-cell embryos from N2 animals treated with control, *top-2* or *capg-2* RNAi were fixed and HCR was performed to probe for F58E6.6 transcripts (white) and DNA (blue). P2 nuclei are outlined with red dashed line while somatic nuclei are outlined by white dashed line. Representative images are shown and quantification of F58E6.6 signal in each blastomere is shown on the right.

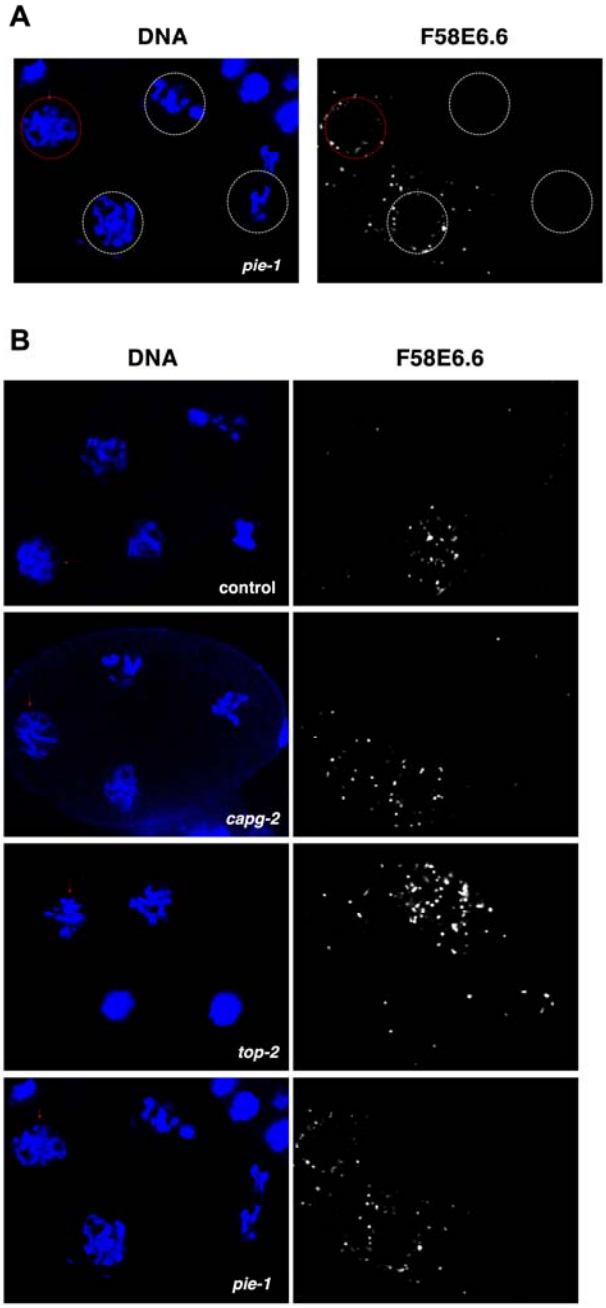

F58E6.6 transcript present in:

P_2	EMS	ABp	ABa
Y	Y	N	N
Y	Y	N	Y
Y	Y	N	N
Y	Y	N	N
Y	Y	N	N
5/5Y	5/5Y	0/5 Y	1/5 Y

C

% of cells expressing F58E6.6 transcript

	P_2	EMS	ABa	ABb	*n*
control	20	100	15	10	20
capg-2	82	100	0	18	11
pie-1	100	100	0	20	5
top-2	50	100	40	40	10

Figure S2: Control experiments for somatic gene expression in 4-cell embryos.

A. Same as Figure 2B except RNAi against *pie-1* was utilized. **B.** The same panels as those shown in Figure 2B are displayed without the dashed circles. **C.** A summary of the data shown in Figures 2B and S2A.

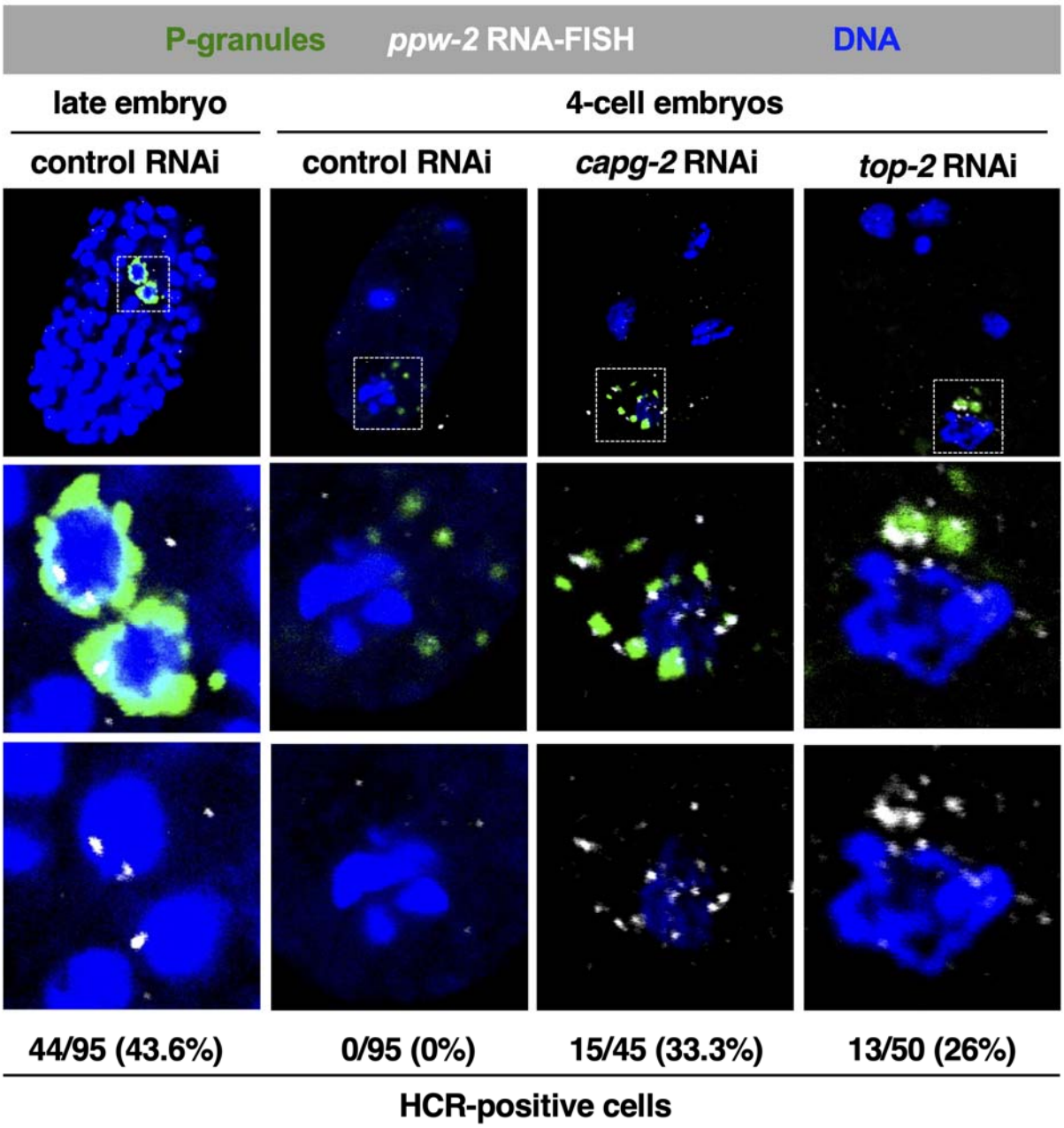

Figure 3: The *ppw-2* transcript is normally expressed in PGCs of late embryos but appears in the P-lineage of early embryos after loss of TOP-2 or CAPG-2.

A strain expressing GFP-tagged PGL-1 (SS747) was used for HCR to detect expression of the *ppw-2* transcript. The left column shows a late embryo, and the Z2/Z3 PGCs are identified via

fluorescence form GFP-PGL-1. Shown in white are the *ppw-2* transcripts. The top image depicts the entire embryo. The middle image is zoomed in on the germ cells and shows both GFP (green) and HCR (white) signals. The bottom image shows just the HCR signal. The remaining columns are the same as the first except these are 4-cell embryos and the P2 blastomere is highlighted. Embryos were derived from animals exposed to the given RNAi. Quantification of the data is provided below the panels.

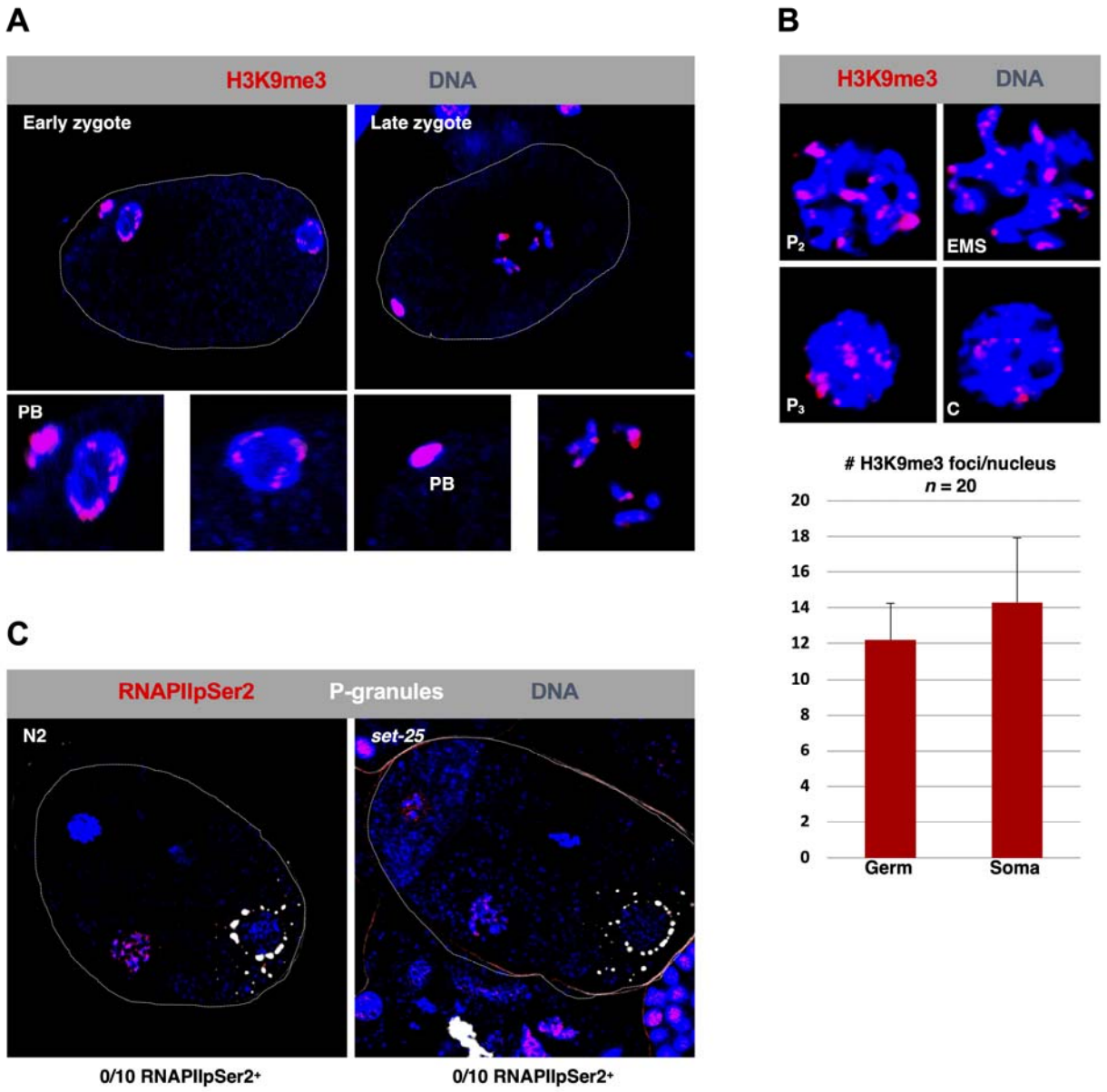

Figure 4: The H3K9me heterochromatin pathway is not required for transcriptional repression in the P lineage.

A. The indicated zygotes from N2 worms were fixed and stained for H3K9me3. Shown below the entire embryos are magnified views of the pronuclei and polar bodies (PB). Note that the H3K9me3 signal overlaps with the DAPI signal more extensively on the polar bodies than within

1 the pronuclei. **B.** Same as (A) except two- and four-cell embryos were examined. Quantification

2 of H3K9me3 foci for P2 and P3 (germ) or EMS and C (soma) is shown below. **C.** Four-cell

3 embryos, either wild type (N2) or *set-25* mutants (strain MT17463), were fixed and stained for

4 RNAPIIpSer2 and P-granules.

5

6

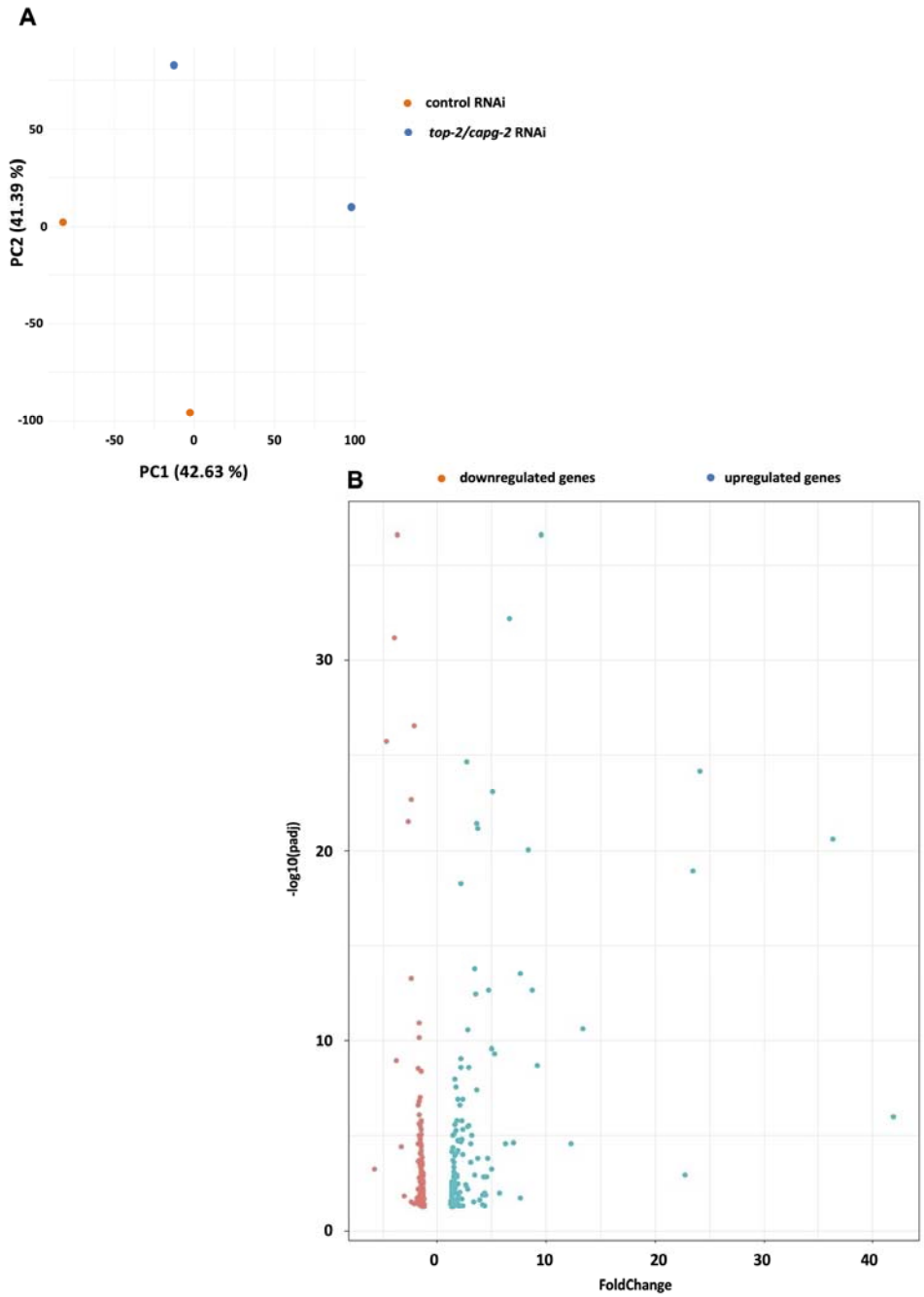

Figure 5: Identification of differentially expressed genes using RNA-seq on control and *top-2/capg-2* RNAi early embryos.

1 **A.** Principle component analysis shows that separation of the data sets is linked to the RNAi

2 that the animals were exposed to. **B.** A volcano plot for the differentially expressed genes. The

3 x-axis shows fold change and the y-axis shows plots adjusted P-values (see Methods).

4

5

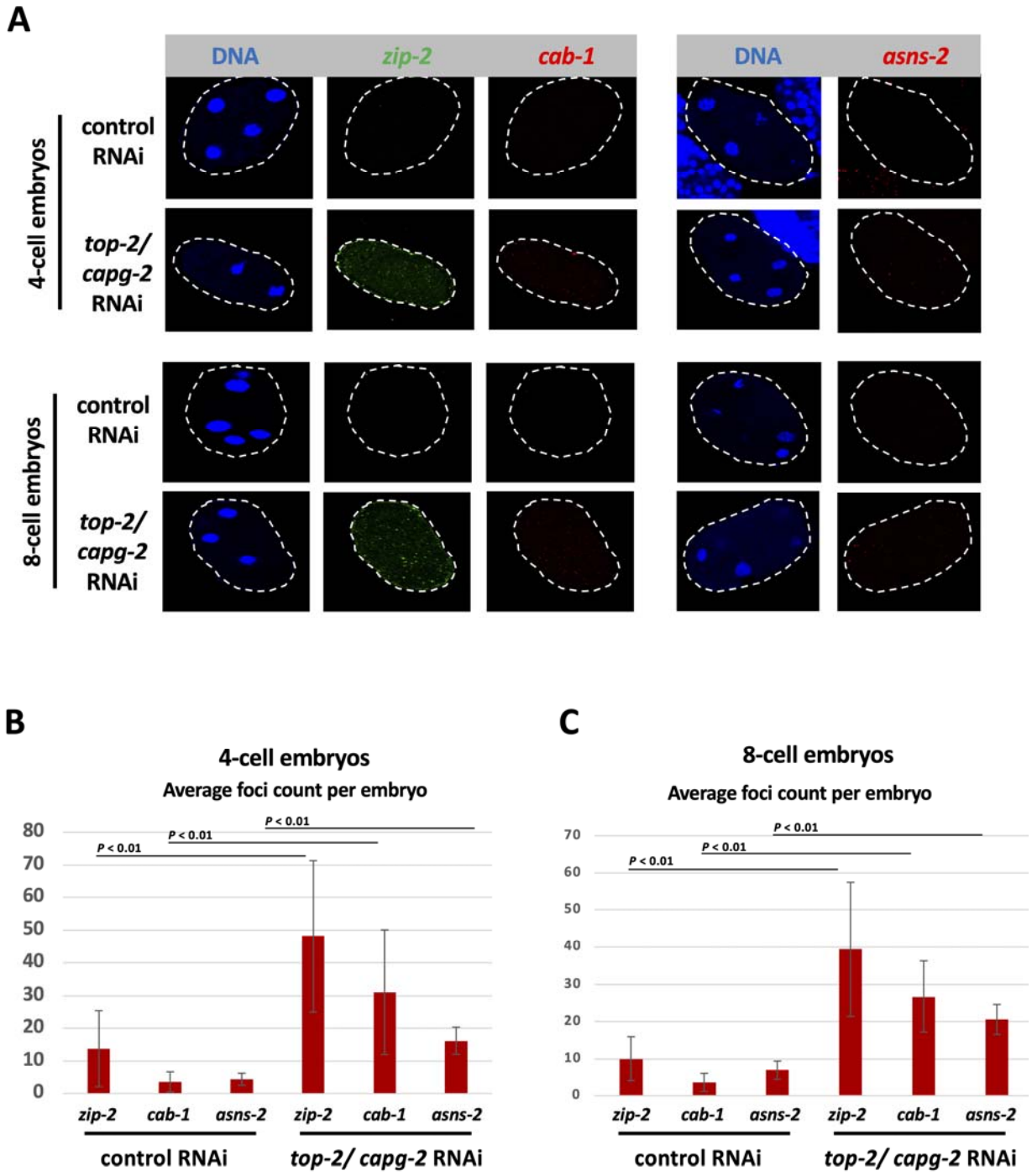

Figure 6: HCR analysis of 3 DEGs in 4- and 8-cell embryos.

A. HCR was performed as in Figures 2&3 with the indicated probes (*zip-2*, *cab-1*, and *asns-2*) on the indicated 4- and 8-cell embryos (either control or *top-2/capg-2* RNAi). Representative

1 images are shown. **B-C.** HCR foci were counted for the indicated samples and their averages are

2 plotted and compared to one another using the Student's t-test.

3

4

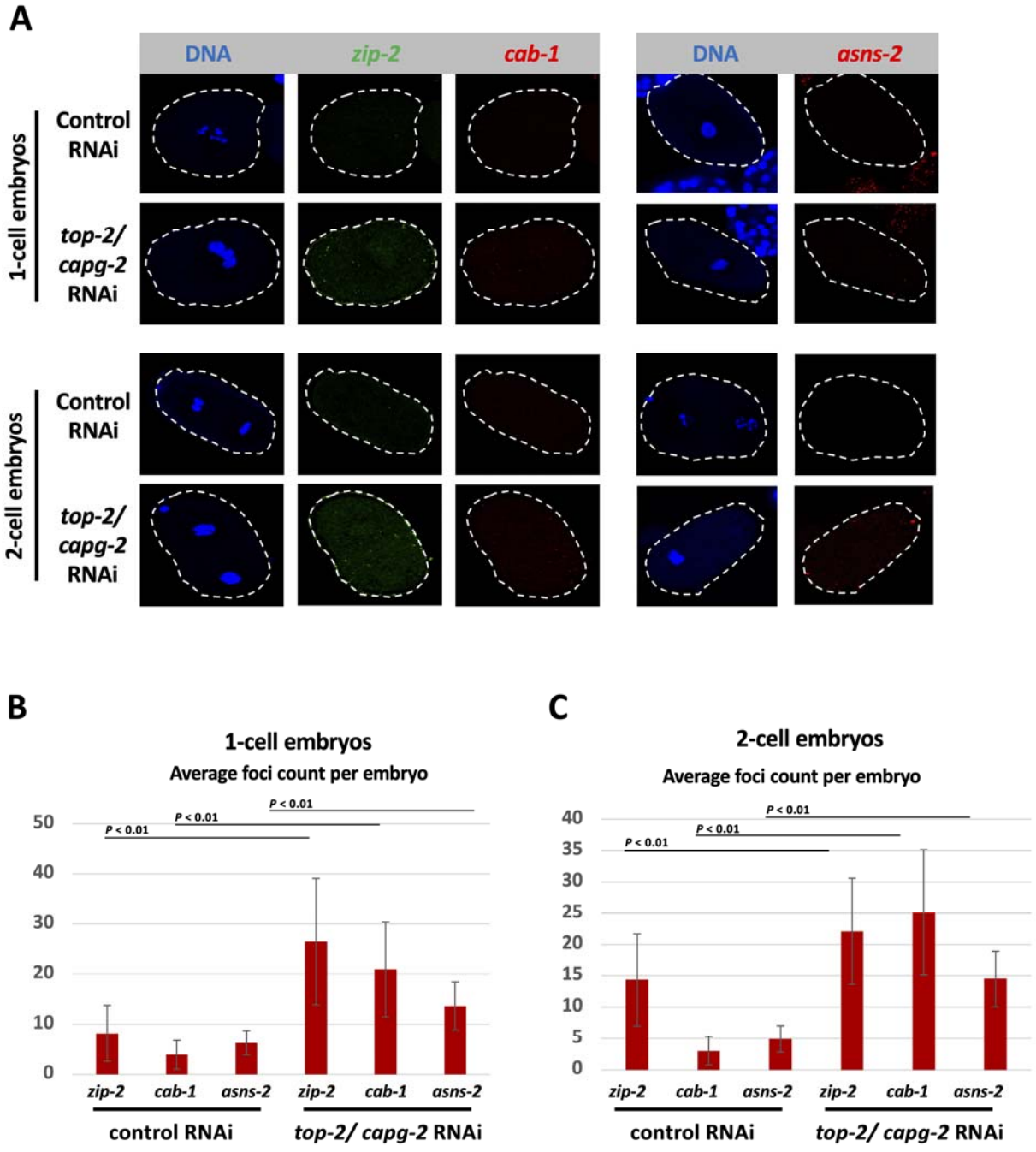

Figure 7: HCR analysis of three DEGs in 1- and 2-cell embryos.

A. HCR was performed as in Figures 2&3 with the indicated probes (*zip-2*, *cab-1*, and *asns-2*) on the indicated 4- and 8-cell embryos (either control or *top-2/capg-2* RNAi). Representative

1 images are shown. **B-C.** HCR foci were counted for the indicated samples and their averages are

2 plotted and compared to one another using the Student's t-test.

3

4

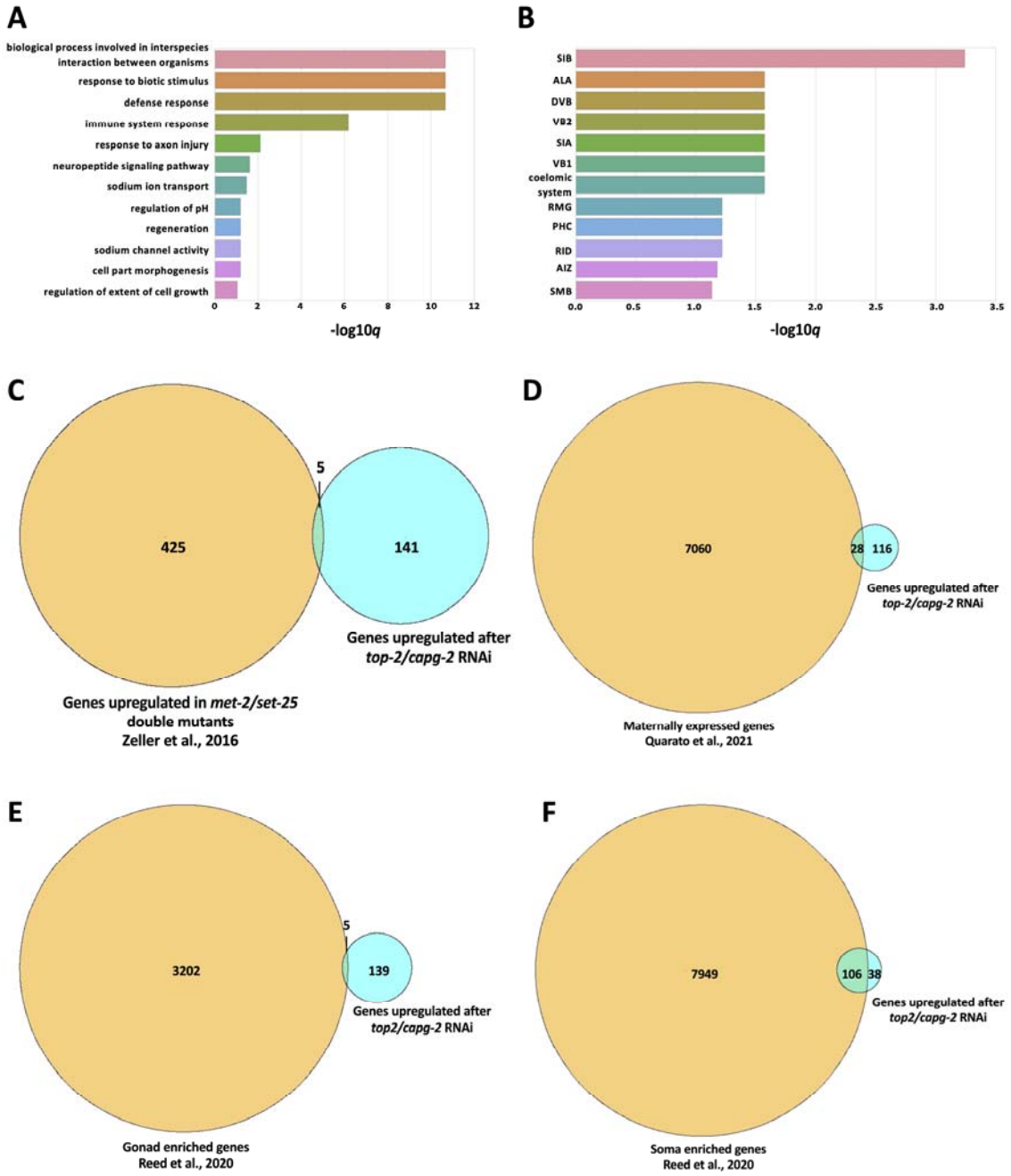

Figure 8: Gene enrichment and overlap analysis for genes upregulated in *top-2/capg-2* RNAi embryos.

A-B. GO (A.) and tissue enrichment (B.) analyses for our set of 144 upregulated genes were performed using the Gene Set Enrichment Analysis tool that is available on Wormbase.org

1 (https://wormbase.org/tools/enrichment/tea/tea.cgi). **C-F.** Overlap analysis for our set of 144

2 upregulated genes was performed against the indicated data sets.